

## Prominent $\beta$ -relaxations in yttrium based metallic glasses

P. Luo, Z. Lu, Z. G. Zhu, Y. Z. Li, H. Y. Bai, and W. H. Wang<sup>a)</sup>

*Institute of Physics, Chinese Academy of Sciences, Beijing 100190, People's Republic of China*

(Received 22 December 2014; accepted 12 January 2015; published online 22 January 2015)

Most metallic glasses (MGs) exhibit weak slow  $\beta$ -relaxation. We report the prominent  $\beta$ -relaxation in YNiAl metallic glass with a wide composition range. Compared with other MGs, the MGs show a pronounced  $\beta$ -relaxation peak and high  $\beta$ -relaxation peak temperature, and the  $\beta$ -relaxation behavior varies significantly with the changes of the constituent elements, which is attributed to the fluctuations of chemical interactions between the components. We demonstrate the correlation between the  $\beta$ -relaxation and the activation of flow units for mechanical behaviors of the MG and show that the MG is model system for studying some controversial issues in glasses. © 2015 AIP Publishing LLC. [<http://dx.doi.org/10.1063/1.4906452>]

Relaxation is one of important routes for understanding the nature of glasses and supercooled liquids.<sup>1</sup> The relaxation behaviors of liquids and glasses are derived from two kinetic processes:<sup>2</sup> a slow process, termed as the  $\alpha$  process, is a large scale irreversible structural rearrangement, and a fast process, termed as the  $\beta$  process, is a locally initiated and reversible process. The slow  $\beta$ -relaxation (also called secondary or Johari-Goldstein relaxation) is an inherent and universal nature of supercooled liquids and glasses<sup>1–6</sup> and is strongly correlated with some key issues in glassy materials and physics such as flow units for flowing in glasses,<sup>7–10</sup> mechanical properties, plastic deformation mechanisms,<sup>9–14</sup> diffusions,<sup>15–17</sup> aging,<sup>18,19</sup> and devitrification in glassy materials.<sup>20–22</sup> As closely connected with the  $\alpha$  process,<sup>23–25</sup> the  $\beta$ -relaxation is an efficient probe in revealing the origin of  $\alpha$ -relaxation,<sup>23–26</sup> and then facilitates the understanding of glass transition.<sup>1,27,28</sup>

In stark contrast to covalent bonded atoms in molecular and polymeric glass-formers, metallic glasses (MGs) are composed of multi-atomic particles, and their structure can be approximately viewed as dense random packing of hard spheres,<sup>29</sup> providing a simple but effective model for the study of  $\beta$ -relaxation. Nevertheless, the most MGs exhibit inconspicuous  $\beta$ -relaxation behavior such as excess wings that almost merge with the  $\alpha$ -relaxations<sup>3,30,33</sup> or broad humps<sup>31–33</sup> which are not prominent enough to be identified. So far, only few MGs such as La-based MGs show distinct loss modulus  $E''$  peak responsible for  $\beta$ -relaxation,<sup>33,35</sup> and the La-based MGs have drawn considerable attention and become one of the current focuses of the research on relaxations as well as its correlation with mechanical and physical properties.<sup>3,7,8,11,25,33–35</sup> However, the glass transition temperature ( $T_g$ ) of La-based MGs is relatively low, just about 150 K above room temperature,<sup>8,33</sup> and the peak temperature of the  $\beta$ -relaxation ( $T_\beta$ ) gets correspondingly low. Consequently, the effect of physical aging dominates even at room temperature, resulting in dramatic change of the properties, and the temperature and time windows of the

La-based MGs for the study of  $\beta$ -relaxation are narrow and not well above room temperature.

In this letter, we report a Y-based MG system showing pronounced  $\beta$ -relaxation peaks which are well separated from the  $\alpha$ -relaxation observed by dynamic mechanical analyzer (DMA). Moreover, the Y-based MGs have much higher  $T_g$  and high thermal stability, which favors the study of  $\beta$ -relaxation in higher and larger temperature and time range. The activation energy of the  $\beta$ -relaxation, the effects of constituent elements on the evolution of  $\beta$ -relaxation, and the correlation between the  $\beta$ -relaxation and the activation of flow units of the Y-based MGs are investigated and compared with other MGs. We demonstrate the correlation between the  $\beta$ -relaxation and the activation of flow units for flowing in glass and show that the MG is a model system for studying some controversial issues in glassy materials.

A series of Y-based metallic glassy ribbons were prepared by a melt spinning method. The glassy nature was ascertained by x-ray diffraction (XRD, a Bruker D8 AA25 diffractometer with the  $Cu K_\alpha$  radiation), and the thermal behaviors were examined by differential scanning calorimetry (DSC) Perkin-Elmer DSC 8000 at a heating rate of 20 K/min. The DMA and tensile stress relaxation were performed on a TA DMA Q800, and tensile method was used in the temperature ramp mode at a heating rate of 3 K/min. For the tensile stress relaxation, to avoid the effect of physical aging and the possible difference among the testing samples induced during the preparation process, all the samples were previously heated up to 5 K above  $T_g$ , isothermal for 3 min, and cooled down in the argon atmosphere prior to the measurements. All the stress relaxation measurements were performed on the specimens at 0.6% tensile strain for 300 min. Before the experiment, a 3 min delay was applied to allow the samples to equilibrate at the testing temperature.

Figure 1(a) shows the XRD pattern of a typical  $Y_{60}Ni_{20}Al_{20}$  MG. The broad diffraction peak without distinct sharp crystalline peaks in the XRD pattern indicates the amorphous structure of the material. The DSC curve of the same sample is illustrated in the inset of Fig. 1(a). The distinct glass transition and sharp crystallization behavior further confirm the glassy structure of the alloy. The  $T_g$  and

<sup>a)</sup> Author to whom correspondence should be addressed. Electronic mail: whw@iphy.ac.cn.

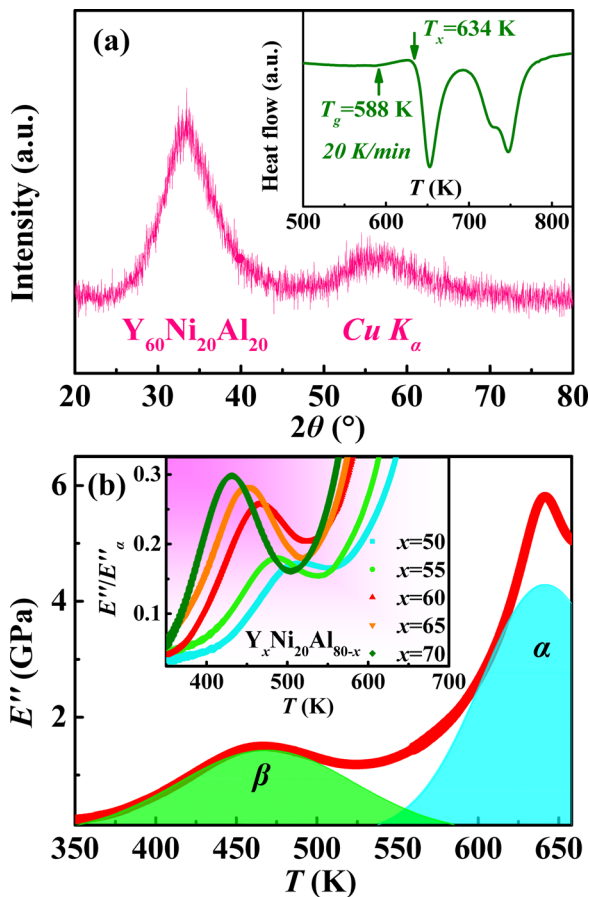


FIG. 1. (a) XRD pattern of  $Y_{60}Ni_{20}Al_{20}$  MG. The inset is the DSC curve of the MG. (b) Temperature dependence of the loss modulus  $E''$  of  $Y_{60}Ni_{20}Al_{20}$  at 1 Hz and a heating rate of 3 K/min. The green and the cyan regions guide the eye to distinguish the  $\beta$ -relaxation from the  $\alpha$ -relaxation. The inset shows the temperature dependent  $E''/E''_{\alpha}$  for  $Y_xNi_{20}Al_{80-x}$  MGs ( $x = 50, 55, 60, 65,$  and  $70$ ) at 1 Hz and 3 K/min, only the  $\beta$ -relaxation peaks are plotted.

crystallization temperature  $T_x$  are 588 K and 634 K, respectively. Its  $T_g$  is about 140 K higher than that of La-based MGs (see Table I). As shown in Fig. 1(b), the temperature dependent loss modulus  $E''$  of a typical  $Y_{60}Ni_{20}Al_{20}$  MG exhibits two distinct peaks: an  $\alpha$ -relaxation peak at  $642 \pm 5$  K and a pronounced  $\beta$ -relaxation peak at  $466 \pm 5$  K. The inset in Fig. 1(b) shows the temperature

TABLE I. Summary of the data of the  $T_g$ , the onset of crystallization temperature  $T_x$  (determined by DSC in a heating rate of 20 K/min), the  $\beta$ -relaxation peak temperature  $T_{\beta}$ , the  $\alpha$ -relaxation peak temperature  $T_{\alpha}$  (measured at 1 Hz), the  $T_{\beta}/T_{\alpha}$ , and the activation energy of  $\beta$ -relaxation  $E_{\beta}$  of  $Y_xNi_{20}Al_{80-x}$  ( $x = 50, 55, 60, 65,$  and  $70$ ),  $La_{60}Ni_{20}Al_{20}$ , and  $Y_{60}M_{15}Al_{25}$  MGs ( $M = Ni, Co, Cu,$  and  $Fe$ ).

Alloy	$T_g$ (K)	$T_x$ (K)	$T_{\beta}$ (K)	$T_{\alpha}$ (K)	$T_{\beta}/T_{\alpha}$	$E_{\beta}$ (kJ/mol)
$Y_{50}Ni_{20}Al_{30}$	655	701	$517 \pm 5$	$682 \pm 5$	0.76	114
$Y_{55}Ni_{20}Al_{25}$	639	669	$488 \pm 5$	$663 \pm 5$	0.74	114
$Y_{60}Ni_{20}Al_{20}$	588	634	$466 \pm 5$	$642 \pm 5$	0.73	117
$Y_{65}Ni_{20}Al_{15}$	...	690	$451 \pm 5$	$694 \pm 5$	0.65	121
$Y_{70}Ni_{20}Al_{10}$	...	699	$431 \pm 5$	$705 \pm 5$	0.61	113
$La_{60}Ni_{20}Al_{20}$	446	495	$357 \pm 5$	$468 \pm 5$	0.76	...
$Y_{60}Ni_{15}Al_{25}$	588	664	$479 \pm 5$	$667 \pm 5$	0.72	...
$Y_{60}Co_{15}Al_{25}$	648	678	$511 \pm 5$	$672 \pm 5$	0.76	...
$Y_{60}Cu_{15}Al_{25}$	...	634	...	$625 \pm 5$	...	...
$Y_{60}Fe_{15}Al_{25}$	667	697	...	$698 \pm 5$	...	...

dependent  $E''/E''_{\alpha}$  ( $E''_{\alpha}$  represents the corresponding maximum of  $E''$  of  $\alpha$ -relaxation peak) of the  $\beta$ -relaxation peaks of  $Y_xNi_{20}Al_{80-x}$  MGs ( $x = 50, 55, 60, 65,$  and  $70$ ) at the same testing condition. As the Y-Al ratio increases, the corresponding peak of  $\beta$ -relaxation shifts to lower temperature and intriguingly becomes sharper.

Figure 2(a) compares the  $\beta$ -relaxation behaviors of  $Y_{60}Ni_{20}Al_{20}$  and another well studied La-based MGs showing a clear  $\beta$ -relaxation peak in its  $E''$  curve. The  $E''$  curves have been scaled for comparison. The temperature is scaled by the peak temperature of  $\alpha$ -relaxation  $T_{\alpha}$ , and the  $E''$  (measured at 1 Hz) is normalized by  $E''_{\alpha}$ . From the normalized plot, one can clearly identify that the  $\beta$ -relaxation of  $Y_{60}Ni_{20}Al_{20}$  MG is much stronger than that of  $La_{60}Ni_{20}Al_{20}$  MG, whether in terms of the normalized intensity of  $E''$  or the extent of the split between the  $\beta$ - and  $\alpha$ -relaxations directly visualized by the scaled temperature.

The behavior of  $\beta$ -relaxation in different MGs varies significantly. Most MGs exhibit as excess wings or broad humps<sup>31–33</sup> that almost merge with  $\alpha$ -relaxation.<sup>3,30,33</sup> For different MGs, their ratio of  $T_{\beta}$  and  $T_{\alpha}$  varies significantly as directly observed from either the measured  $E''$  curves or the Kohlrausch-Williams-Watts (KWW) fits.<sup>15,35</sup> We define  $T_{\beta}/T_{\alpha}$  as a parameter to evaluate the strength of  $\beta$ -relaxation: the smaller the value of  $T_{\beta}/T_{\alpha}$ , the stronger the  $\beta$ -relaxation and vice versa. Figure 2(b) plots the value of  $T_{\beta}/T_{\alpha}$  as a

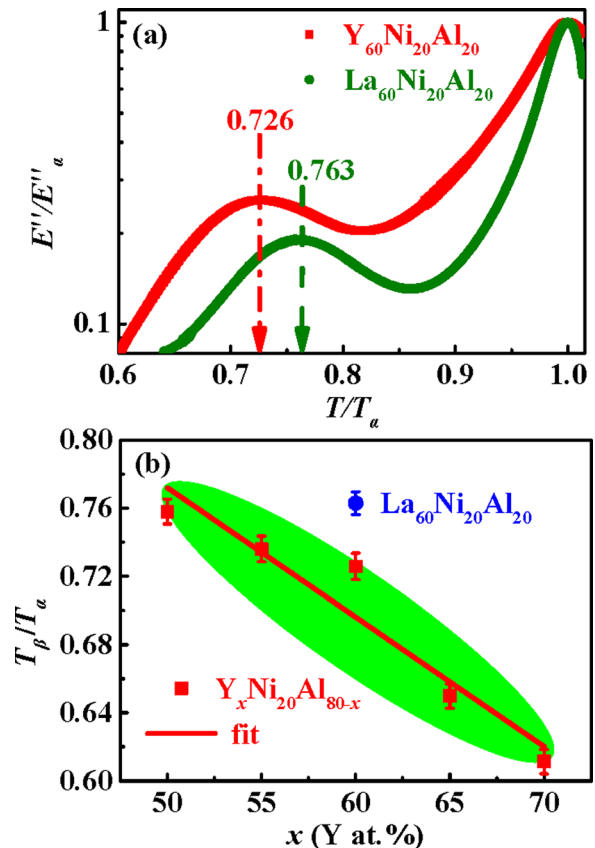


FIG. 2. (a) Comparisons of the  $\beta$ -relaxations of  $Y_{60}Ni_{20}Al_{20}$  and  $La_{60}Ni_{20}Al_{20}$  MGs in a normalized plot,  $T$  scaled by  $T_{\alpha}$  and  $E''$  (measured at 1 Hz) normalized by  $E''_{\alpha}$ . (b) Composition dependent  $T_{\beta}/T_{\alpha}$  for  $Y_xNi_{20}Al_{80-x}$  MGs ( $x = 50, 55, 60, 65,$  and  $70$ ). The line is the best linear fit to the data. The individual dot corresponding to  $La_{60}Ni_{20}Al_{20}$  MG is presented for comparison.

function of Y content (at. %) for  $Y_xNi_{20}Al_{80-x}$  MGs ( $x = 50, 55, 60, 65,$  and  $70$ ). The individual inserted dot corresponding to the  $T_\beta/T_x$  value of  $La_{60}Ni_{20}Al_{20}$  MG is presented for comparison. As the content of Y increases, the  $T_\beta/T_x$  decreases monotonously and remarkably, meaning that the  $\beta$ -relaxations become more pronounced with the increase of the Y–Al ratio in Y-based MGs. In addition, the  $\beta$ -relaxation of Y-based MGs is much stronger than that of La-based MGs with similar rare earth content.<sup>3,7,11,33</sup>

The  $\beta$ -relaxation behaves in Arrhenius type and its activation energy  $E_\beta$  can be determined from  $\ln(f)$  vs  $1000/T_\beta$  plot (Arrhenius plot).<sup>7,33</sup> The peak temperature of the  $\beta$ -relaxation obviously shifts to higher temperature with the frequency increasing from 0.5 to 16 Hz as shown in Fig. 3. The inset in Fig. 3 shows the Arrhenius plots of the peak temperature vs frequency of the  $\beta$ -relaxation for  $Y_xNi_{20}Al_{80-x}$  MGs, and the  $E_\beta$  is determined from these plots, and the data are listed in Table I.

The composition and constituent elements play an important role in the modification of  $\beta$ -relaxation behavior,<sup>34,35</sup> and minor addition or substitution of the elements can result in significant variation in  $\beta$ -relaxation behavior. To understand the mechanism of the pronounced  $\beta$ -relaxation, we investigate the effects of the constituent element on the  $\beta$ -relaxation in the typical Y-based MGs. The results of the substitution of the component Ni by elements with similar atomic radius such as cobalt, copper, and iron are shown in Fig. 4(a). The different constituent elements markedly influence the  $\beta$ -relaxation behavior. The  $Y_{60}Co_{15}Al_{25}$  and  $Y_{60}Ni_{15}Al_{25}$  show similar  $\beta$ -relaxation behavior with a slight change of peak temperature and intensity, while the substitution of copper or iron for nickel leads to the disappearance of the  $\beta$ -relaxation peak: the Y–Cu–Al MG shows a broad hump, and the Y–Fe–Al MG only exhibits an unobvious excess wing in the DMA spectrum. As the Ni, Co, Cu, and Fe have nearly the same atomic radii but different electronic configurations, the intense variation in the  $\beta$ -relaxation behaviors probably arises from the fluctuations of chemical interactions between the constituent elements. It is

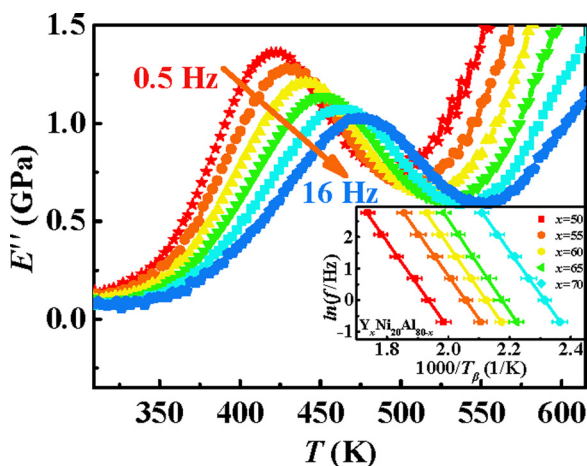


FIG. 3. Temperature dependent  $E''$  at different frequencies, from left to right: 0.5, 1, 2, 4, 8, and 16 Hz (for  $Y_{70}Ni_{20}Al_{10}$  MG). The inset is the Arrhenius plots of  $\ln(f)$  vs  $1000/T_\beta$  for  $Y_xNi_{20}Al_{80-x}$  MG, and the activation energies of  $\beta$  relaxation ( $E_\beta$ ) are determined.

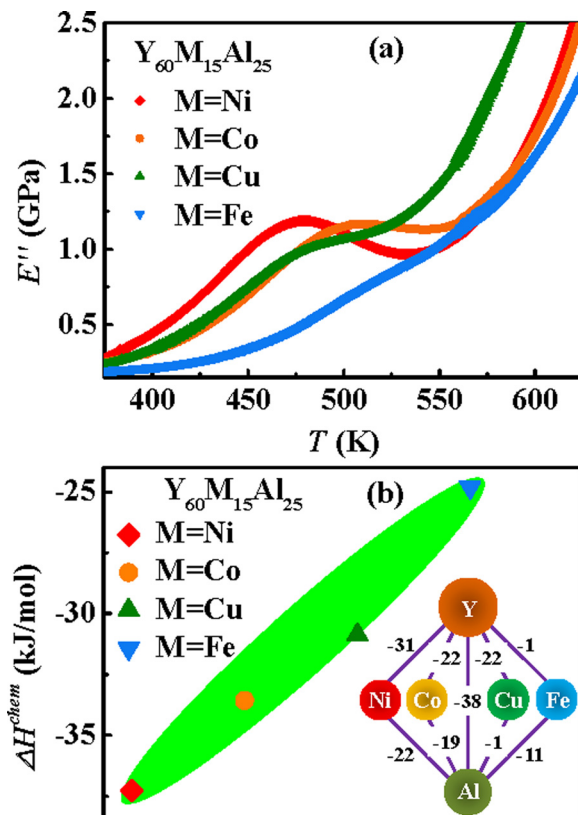


FIG. 4. (a) Temperature dependent  $E''$  (measured at 1 Hz). (b) Composition dependent mean chemical affinity  $\Delta H^{chem}$  of  $Y_{60}M_{15}Al_{25}$  MGs ( $M = Ni, Co, Cu,$  and  $Fe$ ). The inset shows the mixing enthalpy of the constituent atomic pairs in Y–(Ni, Co, Cu, Fe)–Al systems with the unit of kJ/mol.

previously suggested that the  $\beta$ -relaxation behavior in MGs is closely associated with the enthalpy of mixing in the alloys,<sup>34</sup> and the large similar negative enthalpy of mixing among the constituents favors the manifestation of pronounced  $\beta$ -relaxation peaks, whereas positive or large fluctuations in the values of enthalpy of mixing suppress the  $\beta$ -relaxation. Figure 4(b) plots the mean chemical affinity  $\Delta H^{chem}$  of  $Y_{60}M_{15}Al_{25}$  MGs ( $M = Ni, Co, Cu,$  and  $Fe$ ), where  $\Delta H^{chem}$  was estimated via a weighted average approach,  $\Delta H^{chem} = 4 \sum_{A \neq B} \Delta H_{AB}^{mix} c_A c_B$  ( $c_A$  and  $c_B$  refer to the molar percentage of elements A and B, respectively), and the values of enthalpy of mixing  $\Delta H_{AB}^{mix}$  can be derived from Ref. 36 and illustrated in the inset of Fig. 4(b). Among the four MGs, the  $Y_{60}Ni_{15}Al_{25}$  system has the largest negative value of  $\Delta H^{chem}$  and most similar negative enthalpy of mixing, in accordance with the manifestation of the most prominent  $\beta$ -relaxation peak. Compared with  $Y_{60}Ni_{15}Al_{25}$ , the  $\Delta H^{chem}$  of  $Y_{60}Co_{15}Al_{25}$  MG is larger, and the  $\beta$ -relaxation peak gets suppressed. Atomic pair of Y–Cu has a relatively large negative enthalpy of mixing of  $-22$  kJ/mol, but that of the Cu–Al pair is just  $-1$  kJ/mol. The  $\Delta H^{chem}$  of  $Y_{60}Fe_{15}Al_{25}$  is the largest and the values of enthalpy of mixing among the constituents fluctuate more sharply. Correspondingly, its  $\beta$ -relaxation manifests only an excess wing. The results indicate that the bonds between Y–Ni(Co) play a crucial role in the occurrence of the pronounced  $\beta$ -relaxation peak, and the change of  $\beta$ -relaxation behavior agrees fairly well with that of the variation of  $\Delta H^{chem}$  and fluctuation of enthalpy of mixing among the constituents.

The  $\beta$ -relaxations structurally originate from the flow units and are closely bound up with the anelastic and plastic deformation behaviors in MGs.<sup>7,11</sup> The activation of flow units and  $\beta$ -relaxations in MGs are found to be directly related, and the activation energy of the  $\beta$ -relaxation and the average potential-energy barriers of flow units are found nearly equivalent.<sup>9</sup> The peak temperature and intensity of the  $\beta$ -relaxation are closely correlated with the average activation energy and distribution of the flow units in MGs.<sup>7,11,37</sup> Stress relaxation method<sup>38–40</sup> can experimentally investigate the distribution and evolution of the energy barriers of flow units in MGs and then can also reflect the  $\beta$ -relaxation behavior in MGs. The stress relaxations were conducted in  $Y_{60}Ni_{15}Al_{25}$  and  $Y_{60}Fe_{15}Al_{25}$  MGs at the same reduced temperature of  $0.718T_x$  (479 K and 501 K for  $Y_{60}Ni_{15}Al_{25}$  and  $Y_{60}Fe_{15}Al_{25}$  MGs, respectively). Figure 5 represents the activation energy spectra  $P(E)$  of  $Y_{60}Ni_{15}Al_{25}$  and  $Y_{60}Fe_{15}Al_{25}$  MGs based on the activation energy spectrum model,<sup>38,40</sup> and the inset shows the corresponding stress relaxation curves. The YNiAl MG with pronounced  $\beta$ -relaxation relaxes more rapidly and sharply than that of the YFeAl MG with suppressed  $\beta$ -relaxation.  $P(E) \approx -d(\sigma(t)/\sigma(0))/kT$  refers to the total available property change induced by all the activation processes in the energy range from  $E$  to  $E + dE$ , and  $E = kT \ln(\vartheta_0 t)$  is derived from the Arrhenius equation taking  $\vartheta_0$  as the Debye frequency of  $10^{13} \text{ s}^{-1}$ . We can see that the activation energy of YNiAl MG is generally lower than that of YFeAl MG, indicating that the relaxation events (or flow units) are easy to be activated in YNiAl MG. By integrating the activation energy spectra over the initial 10 min, the proportions of the activated flow events can be roughly estimated to be 49% and 28% for YNiAl and YFeAl MGs, respectively. For YNiAl MG with pronounced  $\beta$ -relaxation, it has higher density of the flow units with lower activation energy, and much more flow units can be easily activated in its initial stage compared to that of the YFeAl.<sup>39</sup> Above  $T_\beta$ , a connective percolation state achieves and leads to the excitation of the microscopic flow and cooperative glass-to-liquid transition process. Our observations confirm that the  $\beta$ -relaxation behavior is closely correlated with the

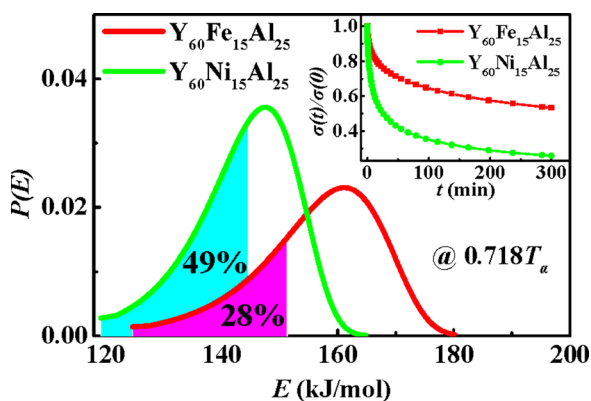


FIG. 5. The activation energy spectra  $P(E)$  of  $Y_{60}Ni_{15}Al_{25}$  and  $Y_{60}Fe_{15}Al_{25}$  MGs. The dashed areas represent the activated flow units over the same initial activation time of 10 min. The inset is the stress relaxation curves of  $Y_{60}Ni_{15}Al_{25}$  and  $Y_{60}Fe_{15}Al_{25}$  MGs at  $0.718T_x$ , and the stress  $\sigma(t)$  is normalized by the initial stress  $\sigma(0)$ .

activation of flow units which control the mechanical behaviors of MGs.

In summary, the YNiAl MG with prominent  $\beta$ -relaxation is developed with a wide composition range, a more pronounced  $\beta$ -relaxation peak, and much higher  $\beta$ -relaxation peak temperature. The base element Y can tune the behavior of the  $\beta$ -relaxation. We find that the  $\beta$ -relaxation behavior varies significantly with the change of constituent elements, and the bonds between Y–Ni(Co) play a crucial role in the occurrence of the pronounced  $\beta$ -relaxation peak. The more similar negative enthalpy of mixing among all the constituent elements favors the pronounced  $\beta$ -relaxation peak, whereas the large fluctuations in the values of enthalpy of mixing suppress the  $\beta$ -relaxation. The reason for pronounced  $\beta$ -relaxation in the MGs is found to be closely correlated with the easier activation of flow units in a MG. The ternary YNiAl MG with a pronounced  $\beta$ -relaxation peak is a model system for studying some long-standing puzzles in glass field and favoring a deeper understanding of the mechanism of relaxations.

The authors are grateful to P. Wen, D. Q. Zhao, D. W. Ding, and M. X. Pan for experimental assistance and discussions. This work was supported by the NSF of China (51271195) and MOST 973 Program (No. 2015CB856800).

<sup>1</sup>K. L. Ngai, *Relaxation and Diffusion in Complex Systems* (Springer, New York, 2011).

<sup>2</sup>G. P. Johari and M. Goldstein, *J. Chem. Phys.* **53**, 2372 (1970).

<sup>3</sup>H. B. Yu, W. H. Wang, and K. Samwer, *Mater. Today* **16**, 183 (2013).

<sup>4</sup>K. L. Ngai and M. Paluch, *J. Chem. Phys.* **120**, 857–873 (2004).

<sup>5</sup>S. Capaccioli, M. Paluch, and K. L. Ngai, *J. Phys. Chem. Lett.* **3**, 735 (2012).

<sup>6</sup>P. Wen, D. Q. Zhao, M. X. Pan, and W. H. Wang, *Appl. Phys. Lett.* **84**, 2790 (2004).

<sup>7</sup>Z. Wang, P. Wen, L. S. Huo, H. Y. Bai, and W. H. Wang, *Appl. Phys. Lett.* **101**, 121906 (2012).

<sup>8</sup>Z. Lu, W. Jiao, W. H. Wang, and H. Y. Bai, *Phys. Rev. Lett.* **113**, 045501 (2014).

<sup>9</sup>H. B. Yu, W. H. Wang, H. Y. Bai, Y. Wu, and M. W. Chen, *Phys. Rev. B* **81**, 220201 (2010).

<sup>10</sup>J. S. Harmon, W. L. Johnson, and K. Samwer, *Phys. Rev. Lett.* **99**, 135502 (2007).

<sup>11</sup>H. B. Yu, W. H. Wang, and H. Y. Bai, *Phys. Rev. Lett.* **108**, 015504 (2012).

<sup>12</sup>R. F. Boyer, *Polym. Eng. Sci.* **8**, 161 (1968).

<sup>13</sup>E. Munch, J. M. Pelletier, and G. Vigier, *Phys. Rev. Lett.* **97**, 207801 (2006).

<sup>14</sup>N. Adachi, Y. Todaka, Y. Yokoyama, and M. Umemoto, *Appl. Phys. Lett.* **105**, 131910 (2014).

<sup>15</sup>H. B. Yu, K. Samwer, Y. Wu, and W. H. Wang, *Phys. Rev. Lett.* **109**, 095508 (2012).

<sup>16</sup>R. Richert and K. Samwer, *New J. Phys.* **9**, 36 (2007).

<sup>17</sup>K. L. Ngai and S. Capaccioli, *J. Phys. Chem.* **138**, 094504 (2013).

<sup>18</sup>R. D. Priestley, C. J. Ellison, and J. M. Torkelson, *Science* **309**, 456 (2005).

<sup>19</sup>J. Hachenberg, K. Samwer, and W. L. Johnson, *Appl. Phys. Lett.* **92**, 131911 (2008).

<sup>20</sup>T. Ichitsubo, E. Matsubara, T. Yamamoto, H. S. Chen, N. Nishiyama, J. Saida, and K. Anazawa, *Phys. Rev. Lett.* **95**, 245501 (2005).

<sup>21</sup>T. Ichitsubo, E. Matsubara, H. S. Chen, J. Saida, T. Yamamoto, and N. Nishiyama, *J. Chem. Phys.* **125**, 154502 (2006).

<sup>22</sup>M. T. Cicerone and J. F. Douglas, *Soft Matter* **8**, 2983 (2012).

<sup>23</sup>R. Boehmer, G. Diezemann, B. Geil, G. Hinze, A. Nowaczyk, and M. Winterlich, *Phys. Rev. Lett.* **97**, 135701 (2006).

<sup>24</sup>K. L. Ngai, *J. Chem. Phys.* **109**, 6982 (1998).

<sup>25</sup>K. L. Ngai, Z. Wang, H. B. Yu, and W. H. Wang, *J. Chem. Phys.* **139**, 014502 (2013).

- <sup>26</sup>R. Casalini and C. M. Roland, *Phys. Rev. Lett.* **102**, 035701 (2009).
- <sup>27</sup>X. Q. Gao, W. H. Wang, and H. Y. Bai, *J. Mater. Sci. Technol.* **30**, 546 (2014).
- <sup>28</sup>J. C. Dyre, *Rev. Mod. Phys.* **78**, 953 (2006).
- <sup>29</sup>W. H. Wang, *J. Appl. Phys.* **99**, 093506 (2006).
- <sup>30</sup>J. C. Qiao and J. M. Pelletier, *J. Mater. Sci. Technol.* **30**, 523 (2014).
- <sup>31</sup>L. N. Hu and Y. Z. Yue, *J. Phys. Chem. C* **113**, 15001 (2009).
- <sup>32</sup>Z. F. Zhao, P. Wen, C. H. Shek, and W. H. Wang, *Phys. Rev. B* **75**, 174201 (2007).
- <sup>33</sup>Z. Wang, H. B. Yu, and W. H. Wang, *J. Phys.: Condens. Matter* **23**, 142202 (2011).
- <sup>34</sup>H. B. Yu, K. Samwer, W. H. Wang, and H. Y. Bai, *Nat. Commun.* **4**, 2204 (2013).
- <sup>35</sup>Z. G. Zhu, K. L. Ngai, and W. H. Wang, *J. Chem. Phys.* **141**, 084506 (2014).
- <sup>36</sup>A. Takeuchi and A. Inoue, *Mater. Trans., JIM* **46**, 2817 (2005).
- <sup>37</sup>W. H. Wang, *J. Appl. Phys.* **110**, 053521 (2011).
- <sup>38</sup>W. Jiao, P. Wen, and W. H. Wang, *Appl. Phys. Lett.* **102**, 101903 (2013).
- <sup>39</sup>Z. Wang, B. A. Sun, H. Y. Bai, and W. H. Wang, *Nat. Commun.* **5**, 5823 (2014).
- <sup>40</sup>H. B. Yu, W. H. Wang, H. Y. Bai, and K. Samwer, *National Sci. Rev.* **1**, 429 (2014).